Electrochimica Acta, 1974, Vol. 19, pp. 583–589. Pergamon Press. Printed in Great Britain

IONIC MASS TRANSFER AT HORIZONTAL DISC ELECTRODES UNDER LONGITUDINAL VIBRATION

J. J. PODESTÁ, G. F. PAÚS and A. J. ARVÍA

Instituto de Investigaciones Fisicoquímicas Teóricas y Aplicadas, División Electroquímica, Facultad de Ciencias Exactas, Universidad Nacional de La Plata, La Plata, Argentina

(*Received* 12 *November* 1973)

Abstract—A dimensionless correlation for ionic mass transfer at horizontal disc electrodes under longitudinal vibration has been obtained. Within a certain range of amplitude and frequency the flow is confined to a cylinder adjacent to the electrode. The fluid boundary layer thickness is rapidly reduced when either the frequency or the amplitude is increased. The longitudinal vibration, under controlled potential conditions, produces an *ac* component in the total current. A comparison of the mass transfer rate equation with others corresponding to different flow regimes reveals that a critical flow rate exists, above which vibration is more efficient than conventional agitation in increasing the mass transfer rate.

NOMENCLATURE

A	electrode area, cm^2
C_0	concentration of the reacting species, mole cm^{-3}
D	diffusion coefficient of the reacting species, $cm^2 s^{-1}$
d	disc diameter, cm
f	frequency, Hz
ΔH_D^*	apparent activation energy for diffusion, kcal $mole^{-1}$
$\Delta H_{I_L}^*$	apparent activation energy for the limiting current, kcal mol^{-1}
ΔH_ν^*	apparent activation energy for viscous flow, kcal $mole^{-1}$
I_L	limiting current, A
K	proportionality constant, $s^{1/4}\,cm^{-1/4}$
$(k_r)_{lam}$	mass transfer coefficient for the rotating disc electrode under laminar flow, $cm\,s^{-1}$
$(k_r)_{tur}$	mass transfer coefficient for the rotating disc electrode under turbulent flow, $cm\,s^{-1}$
k_s	mass transfer coefficient for the stagnation flow electrode, $cm\,s^{-1}$
k_v	mass transfer coefficient for the vibrating electrode, $cm\,s^{-1}$
Re	real part of the exponential function
Re_v	vibrational Reynolds number
r	radial coordinate, cm
Sc	Schmidt number
Sh	Sherwood number
U	flow velocity, $cm\,s^{-1}$
$V(t)$	instantaneous velocity, $cm\,s^{-1}$
$V_{r.m.s.}$	root mean square velocity, $cm\,s^{-1}$
$\Delta x(t)$	normal shift of the disc plane with respect to the rest position, cm
$(\Delta x)_0$	amplitude of the normal shift of the disc plane, cm
$(\Delta x)_{r.m.s.}$	root mean square shift of the disc plane with respect to the rest position, cm
zF	number of coulombs per mole of reacting species
δ_N	Nernst diffusion layer thickness, cm
ν	kinematic viscosity, $cm^2 s^{-1}$
ω	angular frequency s^{-1}

INTRODUCTION

There is a growing interest in the effects of unusual variables, such as oscillations, including vibration and pulsation on transport phenomena. Attention has been directed both towards heat and mass transfer either under steady or non-steady conditions in natural and forced convection [1,2].

Vibrating electrodes are employed in electrochemistry, and particularly in polarography, either as a vibrating dropping mercury electrode [3,4], or as a platinum micro-electrode of different shapes [5–8]. These vibrating electrodes give reproducible polarograms under a certain range of frequency and amplitude. It has also been found that the ionic mass transfer rate under vibration improved by increases in either amplitude or frequency [9,10].

General correlations for mass transfer in vibrating systems have been obtained for the dissolution of benzoic acid cylinders under surface vibration [11], and in diffusion controlled electrolytic processes on cylindrical electrodes under horizontal longitudinal vibration [12].

The relatively scant information which has been so far obtained is insufficient for a general quantitative evaluation of oscillations on transport phenomena in electrode processes, due particularly to the many possible combinations of oscillatory variables, such as frequency, amplitude, direction of oscillation, whether the oscillation is longitudinal or transverse relative to the direction of the flow, whether the oscillation is applied to the fluid or to the surface.

The present report refers to a correlation for ionic mass transfer process occurring at a horizontal disc electrode mounted on a conical shape holder under longitudinal vibration.

EXPERIMENTAL

The electrolysis cell consisted of a double wall Pyrex glass container (Fig. 1) of 300 ml capacity, assembled with the vibrating electrode, the counter electrode and the reference electrode.

The vibrating electrode consisted of a bright platinum disc (either 0·3, 0·6 or 1·5 cm dia), axially placed into the cell. The disc was mounted on the end of an inverted, hollow, truncated cone made of a light insulating material which was attached to the diaphragm of a commercial 7 in. loudspeaker. The disc–loudspeaker unit was assembled at the top of the cell. The electric contact to the platinum disc was made with a platinum wire connected through the interior of the hollow cone. Fresh electrode surfaces were used for each run. The counter electrode was a conventional platinum mesh electrode symmetrically placed around the vibrating electrode. A platinum wire properly shielded served as the reference electrode.

The vibration of the loudspeaker–electrode system was driven with a conventionally amplified *ac* signal from an audiofrequency generator covering 10–200 Hz. The frequency and the r.m.s. excitation potential were accurately checked with conventional meters. The vibration amplitude was measured by optical sampling with a flash-type stroboscope.

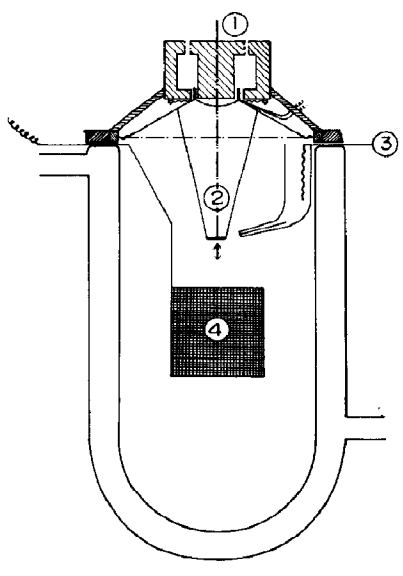

Fig. 1. Scheme of the electrolysis cell: 1 and 2—loudspeaker and disc electrode unity; 3—reference electrode; 4—counter-electrode. The arrows indicate the direction of vibration.

Equimolar aqueous solutions of $[Fe(CN)_6]^{4-}$/$[Fe(CN)_6]^{3-}$ (10^{-3} to 5×10^{-3} M) with different supporting electrolytes (NaOH, KCl) at various concentrations (0·5 and 1 M) were used. Sometimes polyethyleneglycol derivatives (Carbowax, Emkapol 6000) were added at different concentrations to change the viscosity of the solution and the diffusivity of the reacting species. Both the anodic and cathodic average current/potential curves were recorded at a potential sweep rate of 10 mV/s. Runs were made under an inert (N_2) atmosphere and in the temperature range 25 to 40°C, under different vibration frequencies. Instantaneous current displays were pictured from the oscilloscope screen.

Parallel experiments on a platinum rotating disc electrode (*rde*) were made to determine the experimental diffusion coefficient of the reacting species when data was not available. These experiments were also useful for comparing the vibrating electrode characteristics with those of the *rde*, which is well known both from the theoretical and the experimental viewpoints.

Characteristics of vibration

The electrode vibrated sinusoidally normal to the disc plane. The shift $\Delta x(t)$ with respect to the rest position is:

$$\Delta x(t) = (\Delta x)_0 \, Re(e^{j\omega t}) \qquad (1)$$

where $(\Delta x)_0$ is the amplitude and $(\omega = 2\pi f)$ is the angular frequency in s^{-1}. The velocity $V(t)$ associated with the vibration is:

$$V(t) = (\Delta x)_0 \, \omega \, Re(je^{j\omega t}). \qquad (2)$$

As usual, the following expression results for the root mean square velocity, $V_{r.m.s.}$

$$V_{r.m.s.} = \omega(\Delta x)_{r.m.s.}. \qquad (3)$$

The vibration amplitude was changed by varying the excitation potential of the loudspeaker. A symmetrical linear relationship between those magnitudes (in the range 70–800 mV) was established.

Hydrodynamic characteristics of the vibrating electrode

The hydrodynamic profile in the vicinity of the vibrating electrode was visualised by means of a dyeing technique. This was made by adding phenolphthalein to the aqueous electrolyte (0·5 M $NaNO_3$) and cathodising the electrode to a potential slightly lower than that required for the macroscopic evolution of hydrogen. The local increase of pH at the electrode/solution interphase produced a red coloured region around the electrode which indicated the type of flow pattern prevailing there. At 50 Hz when the excitation potential was such that the peak to peak amplitude is lower than 0·11 cm, the coloured liquid film was constrained to a cylinder determined by the disc surface and a height which was of the order of the peak to peak amplitude. At higher excitation potentials

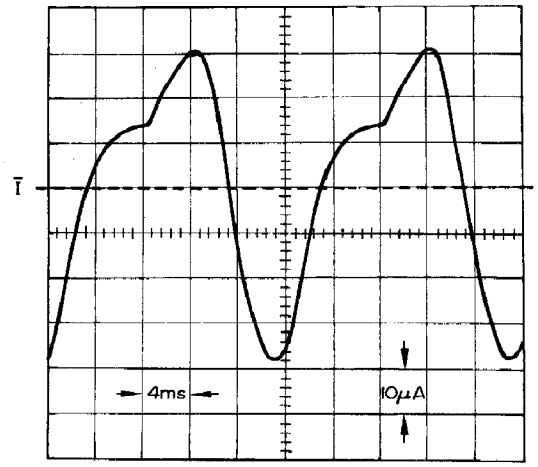

Fig. 2. Current/time display. The horizontal dotted line corresponds to the average current (1·65 mA). $C_{Ferro} = C_{Ferri} = 5 \times 10^{-3}$ M; 0·5 M NaOH; $d = 0{\cdot}6$ cm; 30° C.

(peak to peak amplitude larger than 0·11 cm), the liquid film spread into the electrolytic solution and a net turbulence set in. Most of the runs were made at 50 Hz with a peak to peak amplitude lower than 0·11 cm.

Characteristics of the current flowing through the cell

At the frequencies employed the average electrolysis current was recorded with a conventional ammeter. The current/time display was pictured from the oscilloscope screen. It revealed an *ac* component (Fig. 2) whose amplitude amounted to 1·5 percent of that of the average current. Hence, one can consider that the error due to the current fluctuation lies under

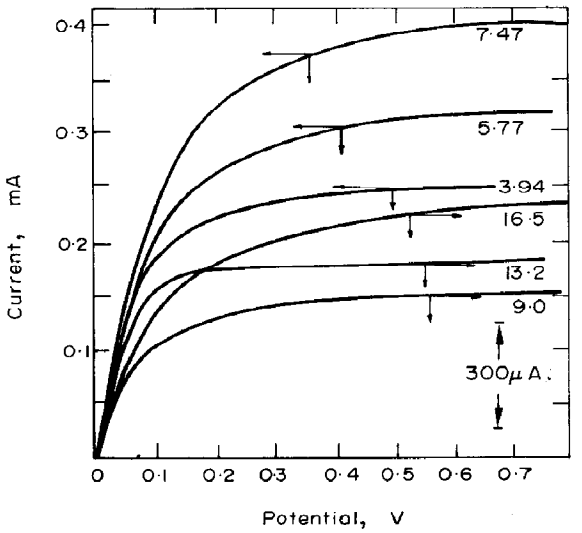

Fig. 3. Average anodic current/potential curves at 50 Hz. $C_{Ferro} = C_{Ferri} = 5 \times 10^{-3}$ M; KCl 0·50 M; $d = 0{\cdot}6$ cm; 30° C. $V_{r.m.s.}$ values in cm s^{-1} are indicated in the figure.

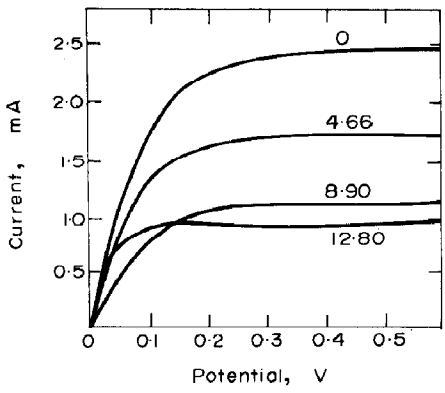

Fig. 4. Average cathodic current/potential curves at 50 Hz and $(\Delta x)_0 = 3{\cdot}68 \times 10^{-2}$ cm. Effect of viscosity. $C_{Ferro} = C_{Ferri} = 5 \times 10^{-3}$ M; 0·5 M NaOH with Emkapol 6000; $d = 1{\cdot}5$ cm. Emkapol concentration per weight is given in the figure.

those errors characterising ionic mass transport experiments. The frequency of the *ac* component corresponded to the vibration frequency although the phase angle was not determined. Its amplitude decreased as the Schmidt number, *Sc*, increased, ($Sc = \nu/D$, where ν is the kinematic viscosity of the solution and D is the diffusion coefficient of the reacting species). The following results refer to the rate of the ionic mass transfer at the vibrating electrode in terms of the average current.

The average current/potential curves. Influence of vibration characteristics

The current/potential curves, either cathodic or anodic, recorded with an X–Y plotter with any of the solutions employed, correspond to those expected for a reversible electrochemical process under convective-diffusion control (Figs. 3 and 4). Under a constant amplitude, within the frequency range from 20 to 100 Hz, the average limiting current increases linearly with the 3/4th power of the frequency. Data shown in Fig. 5 corresponds to runs made with a vibration

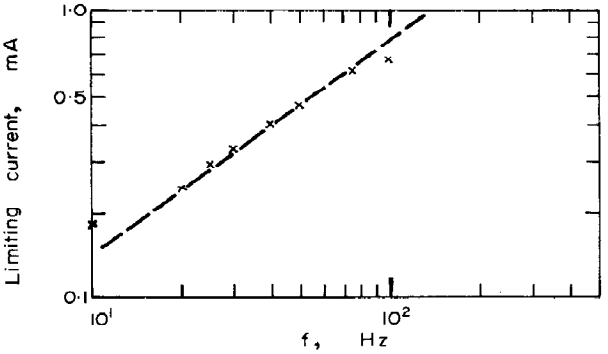

Fig. 5. Dependence of the average cathodic limiting current on vibration frequency at $(\Delta x)_0 = 3{\cdot}68 \times 10^{-2}$ cm. $C_{Ferro} = C_{Ferri} = 5 \times 10^{-3}$ M; 1·008 M NaOH; $d = 0{\cdot}6$ cm; 30° C.

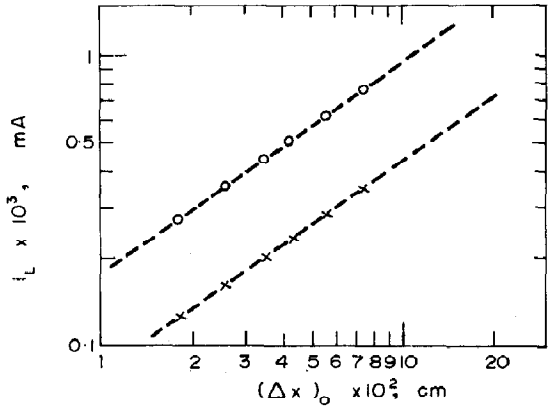

Fig. 6. Dependence of the average limiting current on $(\Delta x)_0$ at 50 Hz. $C_{Ferro} = C_{Ferri} = 5 \times 10^{-3}$ M; 0·5 M KCl; 35°C (○); $C_{Ferro} = C_{Ferri} = 5 \times 10^{-3}$ M; 0·5 M KCl; Carbowax 8 per cent; 30°C (×); $d = 0{\cdot}6$ cm.

amplitude equal to $3{\cdot}68 \times 10^{-2}$ cm. At a constant frequency (50 Hz), the limiting current changes with the vibration amplitude. As seen in Fig. 6, in the range $6{\cdot}35 \times 10^{-3} \leqslant (\Delta x)_0 \leqslant 5{\cdot}5 \times 10^{-2}$, the former depends linearly on the 3/4th power of the vibration amplitude.

Influences of the geometry and solution properties

When the diameter of the vibrating disc at a constant cone angle increases, the limiting current density decreases (Fig. 7) according to a linear $-1/4$th power law. The angle of the supporting hollow cone varies between 0° and 21°. These experiments however are not conclusive since the influence of the cone angle at constant disc diameter was not measured.

Within the experimental errors no detectable influence of the diameter and depth of the cell (between 4–10 cm and 10–25 cm respectively), was found. Any influence of acoustical reflections on the cell inner walls containing the ionic solution must be negligible.

The influence of the ν/D ratio on the limiting current was determined with the 21° angle and 1·5 cm dia electrode using equimolar $(5 \times 10^{-3}$ M) $K_3[Fe(CN)_6] - K_4[Fe(CN)_6]$ solutions (+0·5 M NaOH) with Emkapol 6000 (0–12·8 weight per cent), whose viscosity and diffusion coefficients of the reacting ions are known [13].

The analysis of these results is given below in terms of the dimensionless correlation for the ionic mass transfer process.

A correlation for ionic mass transfer at a vibrating disc

As it is often made in the study of mass transfer at electrodes of complex geometry, it is useful to correlate the results by expressing the data in terms of dimensionless analysis. Considering that a forced flow sets in when the electrode vibrates, it is found:

$$Sh = F(Re_\nu, Sc) \tag{4}$$

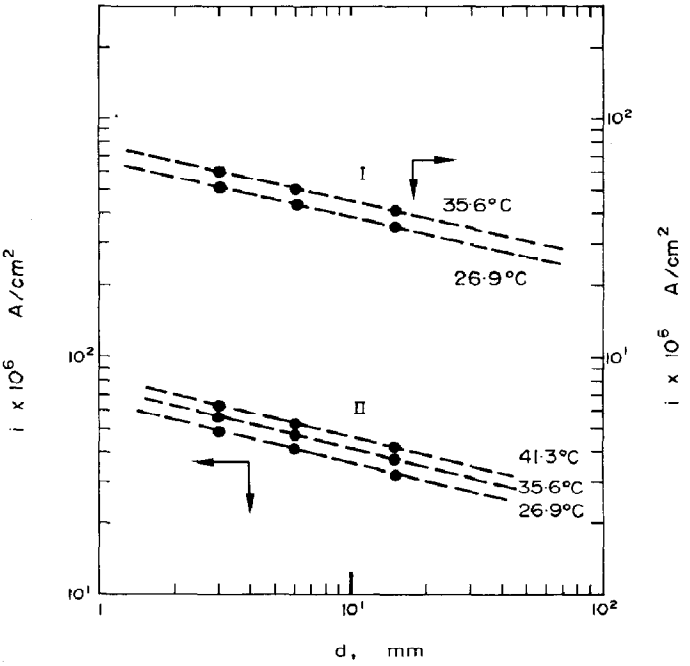

Fig. 7. Dependence of the average limiting current density on vibrating disc diameter at 50 Hz and $(\Delta x)_0 = 5 \times 10^{-2}$ cm. (I) Cathodic runs and (II) anodic runs at different temperatures. $C_{Ferro} = C_{Ferri} = 5 \times 10^{-3}$ M; 1·008 M NaOH.

where Sh and Re_v are the Sherwood's and Reynolds' numbers, respectively. Sh number is:

$$Sh = \frac{I_L d}{AzFC_0 D} \tag{5}$$

where I_L is the limiting current in A; d is the characteristic length in cm which is taken as the disc diameter; A is the electrode area in cm^2; zF is the number of coulombs per mole of reacting species; C_0 is the concentration of the latter in mole cm^{-3} and D its diffusion coefficient in $cm^2 s^{-1}$.

An average Reynolds' number can be defined. If the r.m.s. velocity, $V_{r.m.s.}$, is:

$$V_{r.m.s.} = \frac{\omega(\Delta x)_0}{\sqrt{2}} \tag{6}$$

then an average Re_v number is defined as follows:

$$Re_v = \frac{V_{r.m.s.} d}{\nu}. \tag{7}$$

$V_{r.m.s.}$ is given in $cm\,s^{-1}$ and ν in $cm^2 s^{-1}$.

A plot of log Sh *vs* log Re_v, at constant Sc, yields a straight line with a slope equal to 3/4. This slope keeps reasonably well over the region of Sc numbers covered in these experiments. Analogously, by plotting log Sh against log Sc at constant Re_v a linear relationship is obtained, involving a slope very close to 1/2 (Fig. 8). Consequently, expression (4) can be developed to yield:

$$Sh = 0{\cdot}07\, Re_v^{3/4} Sc^{1/2}. \tag{8}$$

Equation (8) is compared with the experimental results in Fig. 9. This equation is written in terms of I_L as follows:

$$I_L = 0{\cdot}07\, zFAD^{1/2} f^{3/4} (\Delta x)_0^{3/4} \nu^{-1/4} d^{-1/4} C_0. \tag{9}$$

Equation (9) resembles the type of equation already known for ionic mass transfer processes, where a forced convection is provoked either by electrode movement or by the flow of the electrolytic solution. On the basis of equation (9) the results obtained in this work between 25 and 40°C can be easily correlated. The scattering of results is within 4 per cent.

According to equation (9), the temperature dependence of the average limiting current under convective diffusion control yields:

$$\Delta H_{I_L}^* = \tfrac{1}{2}\Delta H_D^* - \tfrac{1}{4}\Delta H_\nu^*, \tag{10}$$

where $\Delta H_{I_L}^*$, ΔH_D^* and ΔH_ν^* are respectively the apparent activation energy for the limiting current, the apparent activation energy for the diffusion process and the apparent activation energy for viscous flow, derived from the experimental variation of viscosity with temperature. Their values are calculated from their corresponding Arrhenius plots (Fig. 10). $\Delta H_{I_L}^*$ is equal to $2{\cdot}7 \pm 0{\cdot}05$ kcal/mole. This figure agrees well with that calculated, according to equation (10), from ΔH_D^* and ΔH_ν^* which are respectively $3{\cdot}65 \pm 0{\cdot}1$ kcal/mole and $-3{\cdot}05 \pm 0{\cdot}05$ kcal/mole.

INTERPRETATION AND DISCUSSION

When edge effects are eliminated by means of a disc whose whole surface is active from the viewpoint of the convective–diffusion process, the vibrating disc electrode behaves in a reproducible manner and it reveals that both the hydrodynamic and the concentration profiles are affected by vibration. Both frequency and amplitude influence the mass transfer rate similarly; vibration increases the mass transfer rate as any other device which produces a decrease of the fluid boundary layer. The layer thickness is radically reduced in a similar fashion to the effect of flow either by electrode rotation or electrolyte flowing on the reacting surface. The longitudinal vibration, however, introduces an *ac* current component in the total current whose magnitude depends on the physicochemical properties of the system, although it represents only a small percentage of the average electrolysis current.

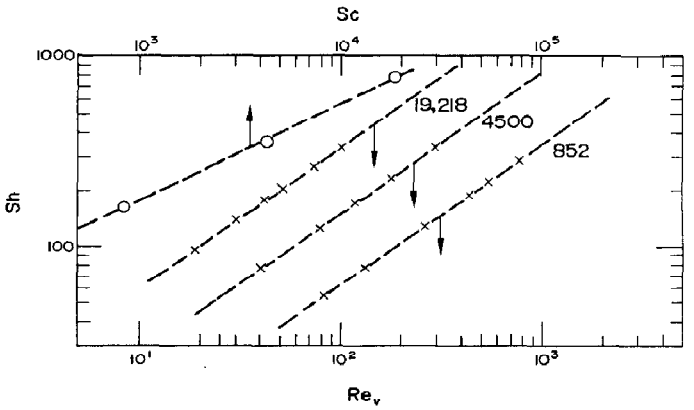

Fig. 8. Log Sh *vs* log Sc plot at $Re_v = 320$, and log Sh *vs* log Re_v plot at different Sc values.

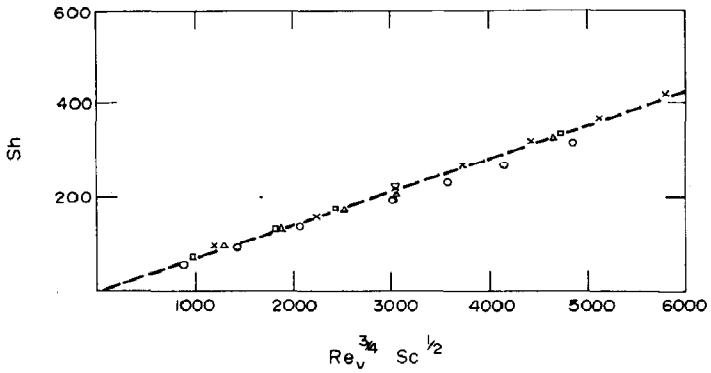

Fig. 9. Plot of the mass transfer correlation as given by equation (8). (○) $C_{Ferro} = C_{Ferri} = 5 \times 10^{-3}$ M; 0·5 M KCl; 35°C. (×) $C_{Ferro} = C_{Ferri} = 5 \times 10^{-3}$ M; 0·5 M KCl; 30°C. (□) $C_{Ferro} = C_{Ferri} = 5 \times 10^{-3}$ M; 0·5 M KCl, Carbowax 4 per cent; 35°C. (△) $C_{Ferro} = C_{Ferri} = 5 \times 10^{-3}$ M; 0·5 M KCl, Carbowax 8 per cent; 35°C.

As the current/time curves were recorded under potentiostatic conditions, the concentration of the reacting species at the electrode surface is constant. Therefore any explanation of the *ac* current component should be related to a variation of the Nernst diffusion layer thickness, δ_N, determined as:

$$\delta_N = \frac{C_0}{(\partial C/\partial x)_{x=0}} \tag{11}$$

when the electrode vibrates. According to equations (9) and (11), for the vibrating electrode:

$$\delta_N = 14{\cdot}3\, D^{1/2}[f(\Delta x)_0]^{-3/4}\nu^{1/4}d^{1/4}. \tag{12}$$

Then, the Nernst diffusion layer thickness depends mainly on the vibration conditions as D and ν can be taken both as constants under the present circumstances due to the low compressibility coefficient of the electrolytic solution.

It seems therefore plausible that the electrode longitudinal vibration produces a significant reduction of δ_N and induces its periodic fluctuation thus causing the *ac* current component to appear. Further discussion of the latter requires additional experimental information concerning the phase angle between the *ac* current component and the proper electrode vibration as well as its dependence on the proper electrode process.

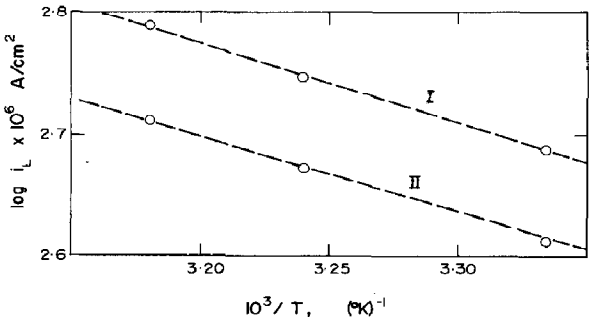

Fig. 10. Arrhenius plots for the anodic limiting current densities determined with two different vibrating electrodes at $V_{r.m.s.} = 10{\cdot}8$ cm s^{-1}. (I) $d = 0{\cdot}3$ cm; (II) $d = 0{\cdot}6$ cm. $C_{Ferro} = C_{Ferri} = 5 \times 10^{-3}$ M; 1·008 M NaOH.

To evaluate the relative efficiency of longitudinal vibration on the mass transfer process a comparison should be attempted between the vibrating electrode and disc electrodes without vibration, such as the flat plate electrode under stagnation flow or the rotating disc electrode, where mass transfer rate equations under different flow regimes have been solved and experimentally tested.

In principle, the hydrodynamic and diffusional pattern of the vibrating electrodes may be approached differently. Thus, if one imagines the disc electrode vibrating at a low frequency and at a large amplitude, the velocity and concentration profiles during the half-cycle, corresponding to its impingement into the solution, may be comparable to those already known for the flat plate electrode under stagnation flow.

This comparison can be attempted in terms of the mass transfer coefficients k_v and k_s, corresponding respectively to the vibrating and the stagnation flow electrodes, which are given respectively by:

$$k_v = 0{\cdot}07\, D^{1/2}[f(\Delta x)_0]^{3/4}\nu^{-1/4}d^{-1/4} \tag{13}$$

and

$$k_s = 0{\cdot}78\, D^{2/3}U^{1/2}(rv)^{-1/2}\nu^{1/3}. \tag{14}$$

U is the flow velocity in cm s^{-1} and r the radial coordinate [14].

These equations produce:

$$\frac{k_v}{k_s} = KU^{1/4}. \tag{15}$$

If $f(\Delta x)_0$ is taken in the vibrating electrode as a linear velocity in cm s^{-1}, K depends on the properties of the solution and geometry. Taking $D = 5{\cdot}95 \times 10^{-6}$ cm^2 s^{-1}, $r = 0{\cdot}3$ cm, $\nu = 8{\cdot}52 \times 10^{-3}$ cm^2 s^{-1}, $K = 1{\cdot}97$ (s cm^{-1})$^{1/4}$, at $U = 2$ cm s^{-1} $= f(\Delta x)_0$, $(k_v/k_s) = 2{\cdot}34$

and at $U = 20\,\text{cm s}^{-1} = f(\Delta x)_0$, $(k_v/k_s) = 4{\cdot}61$. The efficiency, therefore, increases with the $f(\Delta x)_0$ product.

A similar comparison although less realistic, can be made with respect to the rotating disc electrode both under laminar and turbulent flow regimes [15]. The simplest equation for the mass transfer coefficients are:

$$(k_r)_{lam} = 0{\cdot}62\,D^{2/3}\,U^{1/2}r^{-1/2}\nu^{-1/6} \qquad (16)$$

for laminar flow, and:

$$(k_r)_{tur} = 1{\cdot}33\times10^{-3}\nu^{-1/4}D^{3/4}r^{-1}\,U^{0{\cdot}9}r^{0{\cdot}9}\nu^{-0{\cdot}9} \qquad (17)$$

for turbulent flow. From equations (13) and (16), for the system whose characteristics are mentioned above, one obtains: $k_v/(k_r)_{lam} = 2{\cdot}92$ at $U = 2\,\text{cm s}^{-1}$, and $k_v/(k_r)_{lam} = 5{\cdot}20$ at $U = 20\,\text{cm s}^{-1}$. Similarly from equations (13) and (17): $k_v/(k_r)_{tur} = 13{\cdot}3$ at $U = 2\,\text{cm s}^{-1}$ and $k_v/(k_r)_{tur} = 9{\cdot}42$ at $U = 20\,\text{cm s}^{-1}$.

The different ratios of the mass transfer coefficients at constant flow indicate that in the range investigated, the efficiency of the vibrating electrode is greater than the efficiencies of both disc electrodes. They also imply the existence of a critical flow velocity from which the efficiency of the vibrating electrode becomes equal to that of the reference system, so that at flow velocities lower than the critical value the efficiency of the vibrating disc electrode is lower than the efficiencies of those electrodes used for comparison. The existence of a critical linear velocity value may explain some of the discrepancies reported in the literature on the effect of oscillations on transfer coefficients.

Another interesting fact results when comparing the mass transfer coefficients for each particular system at a definite flow velocity. The corresponding ratios are assembled in Table 1. The ratio corresponding to the vibration disc electrode lies between the figures corresponding to the electrodes under laminar flow regime and turbulence flow regime. This indicates that the hydrodynamic and concentration profiles in the case of the vibrating electrode is rather complex. Under the conditions employed in this experiment the situation may be better described as a flow regime in a cylindrical box [16], with a superimposed longitudinal vibration which causes the *ac* current component.

Table 1

System	U cm s^{-1}	$k\times10^4$ cm s^{-1}	Ratio
Long. vibrating disc	2	10·7	5.64
	20	60·4	
Disc (stagnation flow)	2	4·58	3.16
	20	14.5	
Rotating disc (laminar)	2	3·67	3.16
	20	11.6	
Rotating disc (turbulent)	2	0·81	7·91
	20	6.41	

The comparison between the mass transfer coefficients of the vibrating and the rotating disc electrodes are also useful to explain the failure to correlate data obtained at $V_{r.m.s.}$ values larger than $15\,\text{cm s}^{-1}$. For a rotating disc of the same radius this linear velocity is equivalent to a rotation speed of about 500 rev/min. At such a speed, the indicator reaction at a bright platinum electrode is governed by an intermediate kinetics [17]. Therefore, those results obtained at large values of $V_{r.m.s.}$ may not fit equation (9).

In conclusion, a vibrating disc electrode is highly efficient from the viewpoint of increasing the rate of ionic mass transfer. These results encourage further work on the kinetic effects of different vibrations, their interaction with the electrode processes and the characteristics of the *ac* current component, on the theoretical basis for the ionic mass transfer rate equation and on possible applications of vibrating electrodes to different electrochemical processes.

Acknowledgements—This work is part of the research program of the Electrochemistry Division of INIFTA, which is sponsored by the Universidad Nacional de La Plata, the Consejo Nacional de Investigaciones Científicas y Técnicas and the Comisión de Investigaciones Cietíficas de la Provincia de Buenos Aires. J. J. Podestá acted as a Faculty Member of the Departamento de Ingeniería Química de la Universidad Nacional de La Plata. Authors are indebted to Dr. F. Coeuret of the C.N.R.S., Villers-Nancy, France, for the samples of Emkapol 6000.

REFERENCES

1. R. Lemlich, *Chem. Engng* **68**, 171 (1961).
2. R. Lemlich and M. R. Levy, *Am. Inst. chem. Engng J.* **7**, 240 (1961).
3. R. E. Cover, *Reviews in Analytical Chemistry* p. 141. Freund Publishing, Tel Aviv (1972).
4. J. Heyrovsky and J. Kuta, *Principles of Polarography*. Academic Press, New York (1966).
5. E. D. Harris and A. J. Lindsey, *Nature* **162**, 413 (1948).
6. A. J. Lindsey, *J. Phys. Chem.* **56**, 439 (1952).
7. E. D. Harris and A. J. Lindsey, *Analyst* **76**, 647 (1951).
8. E. R. Roberts and J. S. Meek, *Analyst* **77**, 43 (1952).
9. R. Wall and L. C. F. Blackman, *Nature* **202**, 285 (1964).
10. T. K. Ross and A. F. Aspin, *Corros. Sci.* **13**, 53 (1973).
11. K. Somasundara Rao, G. J. V. Jagannadha Raju and C. Venkata Rao, *Indian J. Technol.* **3**, 38 (1965).
12. K. Somasundara Rao, G. J. V. Jagannadha Raju and C. Venkata Rao, *Ind. Chem. Eng.* **5**, 100 (1963).
13. F. Coeuret, private communication.
14. S. L. Marchiano and A. J. Arvia, *Electrochim. Acta* **12**, 801 (1967).
15. B. Levich, *Physicochemical Hydrodynamics*. Prentice-Hall, Englewood Cliffs, New Jersey (1962).
16. D. Groehne, *Nachr. Akad. Wiss. Goettingen*, Math-physik. KI, IIA (1956).
17. J. C. Bazán, S. L. Marchiano and A. J. Arvía, *Electrochim. Acta* **12**, 821 (1967).